



# Nanoparticle-based flow virometry for the analysis of individual virions

Anush Arakelyan, Wendy Fitzgerald, Leonid Margolis, and Jean-Charles Grivel

Program in Physical Biology, Eunice Kennedy-Shriver National Institute of Child Health and Human Development, NIH, Bethesda, Maryland, USA.

**While flow cytometry has been used to analyze the antigenic composition of individual cells, the antigenic makeup of viral particles is still characterized predominantly in bulk. Here, we describe a technology, “flow virometry,” that can be used for antigen detection on individual virions. The technology is based on binding magnetic nanoparticles to virions, staining the virions with monoclonal antibodies, separating the formed complexes with magnetic columns, and characterizing them with flow cytometers. We used this technology to study the distribution of two antigens (HLA-DR and LFA-1) that HIV-1 acquires from infected cells among individual HIV-1 virions. Flow virometry revealed that the antigenic makeup of virions from a single preparation is heterogeneous. This heterogeneity could not be detected with bulk analysis of viruses. Moreover, in two preparations of the same HIV-1 produced by different cells, the distribution of antigens among virions was different. In contrast, HIV-1 of two different HIV-1 genotypes replicating in the same cells became somewhat antigenically similar. This nanotechnology allows the study of virions in bodily fluids without virus propagation and in principle is not restricted to the analysis of HIV, but can be applied to the analysis of the individual surface antigenic makeup of any virus.**

## Introduction

About 50 years ago, flow cytometry revolutionized biology and medicine in general, and immunology in particular, by making possible the distinction of individual cells by their antigenic spectra (1, 2). As a result of this technology, where once we saw only two types of lymphocytes, T and B, we can now recognize dozens of types and hundreds of their states, gaining unprecedented new insights into mechanisms of immunity, including responses to infection by viruses.

Unlike lymphocytes, viruses themselves are still characterized predominantly in bulk, despite the idea that viral particles are probably as individualized as lymphocytes.

Because of its high mutation rate, HIV-1 is one of the most diverse human viruses. Its diversity was recently emphasized by the discovery that only one or several among billions of HIV-1 particles in the seminal fluid of an infected individual are sexually transmitted and start infection in the recipient (3), implying that this transmissible virus is somewhat different from other viral particles, particularly in the composition of its envelope. In order to target these particular viral particles with a new generation of antiviral drugs, one has to be able to characterize these particles individually. Moreover, it appears that the contribution of various infected cells to HIV-1 production depends on the stage of HIV disease and on the presence of opportunistic infection (4). The exact tracing of virions to the cells that have produced them also requires the analysis of individual viral particles. Currently, the envelope composition of viruses is studied by analyzing viral preparations in bulk, although attempts to visualize viruses using flow cytometers have been made (5–9).

The direct use of flow cytometers for viral analysis is hindered by physical limitations (10), since many viruses, especially small RNA viruses like HIV-1 with a diameter of 100 nm, are well outside the light-scattering detection range of commercial cytometers (8). To

overcome this limitation, viruses have been stained with fluorescent nucleic dyes. However, again, small RNA viruses such as HIV could not be detected with this approach, owing to their small genome size (9). Flow cytometry has also been used to quantify viral particles attached to microbeads, which provide light-scattering signal, while viruses were revealed by specific antiviral fluorescent antibodies (11–13). In these assays, multiple viruses attach to one bead, thus such techniques constitute another bulk analysis of viruses. No technology is currently available that is capable of characterizing the antigenic composition of individual viral particles.

Here, we report on such a technology, “flow virometry,” which allows the detection and characterization of antigens on individual virions using multicolor flow analysis. This new method is a technical advance that will help address the question of viral infectivity and transmissibility at the level of a single viral particle.

## Results

*Detection of antigens on individual viral particles: the strategy.* The technology we developed is based on (a) attaching virions to magnetic nanoparticles (MNPs); (b) staining virions immobilized on MNPs with fluorescent antibodies against antigens of interest; (c) separating the resultant complexes from free fluorescent antibodies; and (d) detecting antigens on individual viral particles with regular flow cytometers, in which the triggering event is fluorescence rather than light scattering (Figure 1).

We tested this technology by analyzing the distribution of cellular proteins that previous bulk analyses have shown to be incorporated into HIV-1 virions upon their budding from infected cells. We found that different sets of cellular antigens are distributed differently among individual virions released by infected cells.

*Binding virions to nanoparticles and revealing them by their antigens.* We used 15-nm MNPs formed from iron oxide cores derivatized with carboxyl groups. These particles were coupled to capture antibodies against HIV-1 gp120, either 2G12 (14) or VRC01 (Figure 1, i, and ref. 15). These antibody-coupled MNPs were incubated with HIV-1 suspension (Figure 1, ii), and captured virions were further

**Conflict of interest:** The authors have declared that no conflict of interest exists.

**Citation for this article:** *J Clin Invest.* 2013;123(9):3716–3727. doi:10.1172/JCI67042.

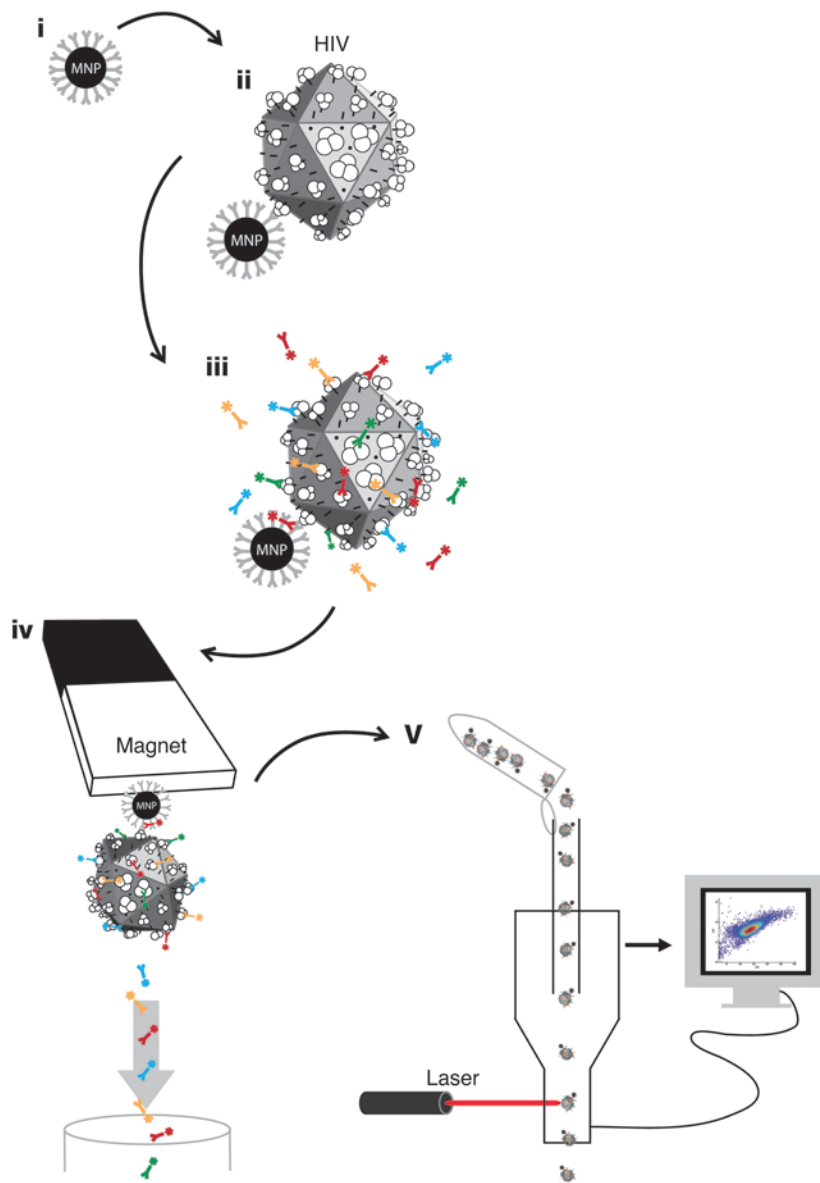


**Figure 1**

Outline of the flow virometry procedure. (i) MNPs coupled to a virion-specific antibody against gp120 (capture antibody, light gray). (ii) MNPs coupled to capture antibody are incubated with viruses (schematically presented as icosahedrons), which become immobilized on MNPs. (iii) MNP-immobilized viruses are visualized with human anti-gp120 antibody (blue) recognizing an epitope different from the one recognized by the capture antibody. MNPs are visualized with a fluorescent antibody or its Fab (red) against the Fc portion of the capture antibody, and viral antigens of interest are visualized with fluorescently labeled monoclonal antibodies (green and yellow). (iv) Virus-MNP complexes with bound antibodies are separated from unbound antibodies with magnetic columns. (v) The MNP-immobilized virions stained with fluorescence-labeled antibodies eluted from the magnetic columns are analyzed with the flow cytometer set up to trigger on MNP fluorescence rather than on light scatter.

studied for the presence of specific antigens. In addition, to visualize MNP–capture antibody complexes, we used fluorescent Fab fragments (Alexa Fluor 488) of goat anti-human IgG antibodies.

We analyzed the presence on the viruses of two cellular antigens, HLA-DR and LFA-1. These antigens were chosen because bulk analysis of HIV-1 preparations has revealed that they are associated with HIV-1 (16, 17). To distinguish virions from microvesicles that have originated from infected cells and therefore may carry viral antigens, we used CD45, which is excluded from virions (18). We incubated HIV-1-MNP complexes with fluorescence-labeled antibodies against the above-mentioned antigens (Figure 1, iii) and isolated the resultant complexes. We used magnetic columns for the removal of unbound fluorescent antibodies from those bound to the HIV-1-MNP complexes, which is critical for flow analysis, as these antibodies cannot be distinguished from each other on the basis of their fluorescence. After the antibody-labeled HIV-1-MNP complexes were immobilized on the column in a magnetic field, we washed the column to remove unbound fluorescent antibodies

(Figure 1, iv). Then, we eluted the antibody-labeled HIV-1-MNP complexes from the column outside the magnetic field and subjected them to analysis with a flow cytometer (Figure 1, v).

*Flow analysis of virions.* We set up the flow cytometer to be triggered by the fluorescent label of the MNP and tested different flow rates to acquire samples. We chose a flow rate below 150 events per second, which, on the basis of earlier reports (19), we expected (and proved below) to resolve individual particles. We used a gate of fluorescence width versus height to exclude aggregates (Figure 2A). Next, we excluded microvesicles bound to MNPs based on their expression of CD45, which is excluded from viral particles (18) (Figure 2B). We visualized HIV-1-MNP complexes with an Alexa Fluor 647-labeled antibody against gp120, which was different from the antibody through which the virions had been captured (Figure 2C). On average,  $90.6\% \pm 6.3\%$  ( $n = 7$ ) of the events were positive for fluorescent anti-gp120 antibodies and negative for CD45.

To verify that the events we registered with the flow cytometer were indeed viral particles and that these events predominantly

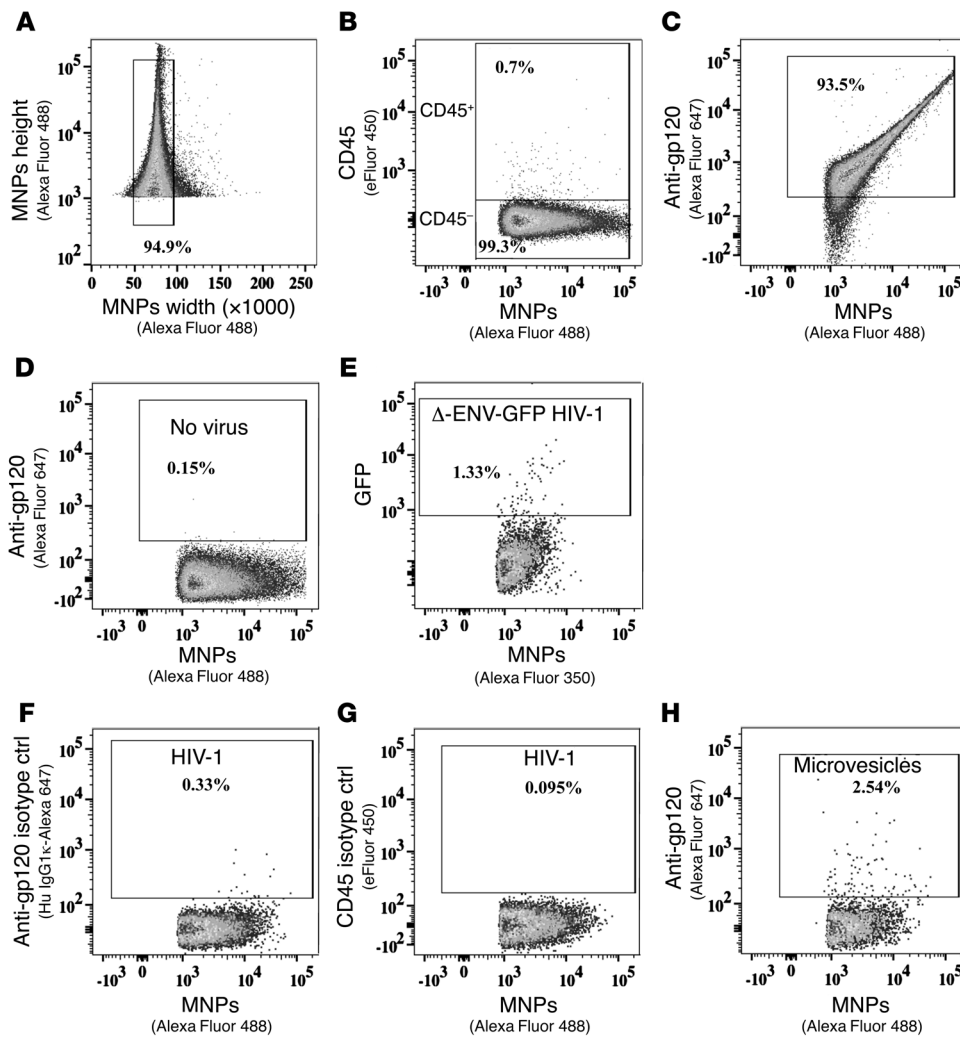


**Figure 2**

Detection of HIV-1 virions immobilized on MNPs. (A) Gating strategy for flow analysis of MNP complexes: A singlet gate was defined by plotting fluorescence height versus fluorescence width. The gate excludes events with a high width and high height that represent aggregated particles (for more details on gating, see Supplemental Figure 1. Supplemental material available online with this article; doi: 10.1172/JCI67042). (B and C) 2G12-coupled MNPs labeled with Alexa Fluor 488 were incubated with HIV-1<sub>SF162</sub> and stained with Alexa Fluor 647-labeled anti-gp120 antibody VRC01, and eFluor 450-labeled anti-CD45 antibody. CD45-positive events (B) are excluded from analysis, while gated CD45-negative MNP events positive for VRC01 (C) represent HIV-1 bound to the MNPs. (D) 2G12-coupled MNPs labeled with Alexa Fluor 488 were incubated with virus-free culture medium and stained with Alexa Fluor 647-labeled anti-gp120 antibody VRC01. Note the very low nonspecific binding of anti-gp120 antibodies to MNPs. (E) 2G12-coupled MNPs labeled with Alexa Fluor 350 were incubated with Δ-ENV-GFP HIV-1. Note the low binding of Δ-ENV-GFP HIV-1 to MNPs. (F–H) 2G12-coupled MNPs labeled with Alexa Fluor 488 were incubated with HIV-1<sub>SF162</sub> and stained with Alexa Fluor 647-labeled human IgG1 (Hu IgG1) (F) or eFluor 450-labeled IgG1 κ (G) isotype control antibodies for gp120 or CD45, respectively. Note the very low nonspecific binding of isotype control (ctrl) antibodies to HIV-1-MNP complexes. (H) 2G12-coupled MNPs labeled with Alexa Fluor 488 were incubated with a suspension of microvesicles produced by uninfected cells and stained with Alexa Fluor 647-labeled anti-gp120 antibody VRC01. Note the low binding of MNPs to microvesicles. On each plot, the fraction of events in their respective gate is expressed as a percentage of the total events in the plot.

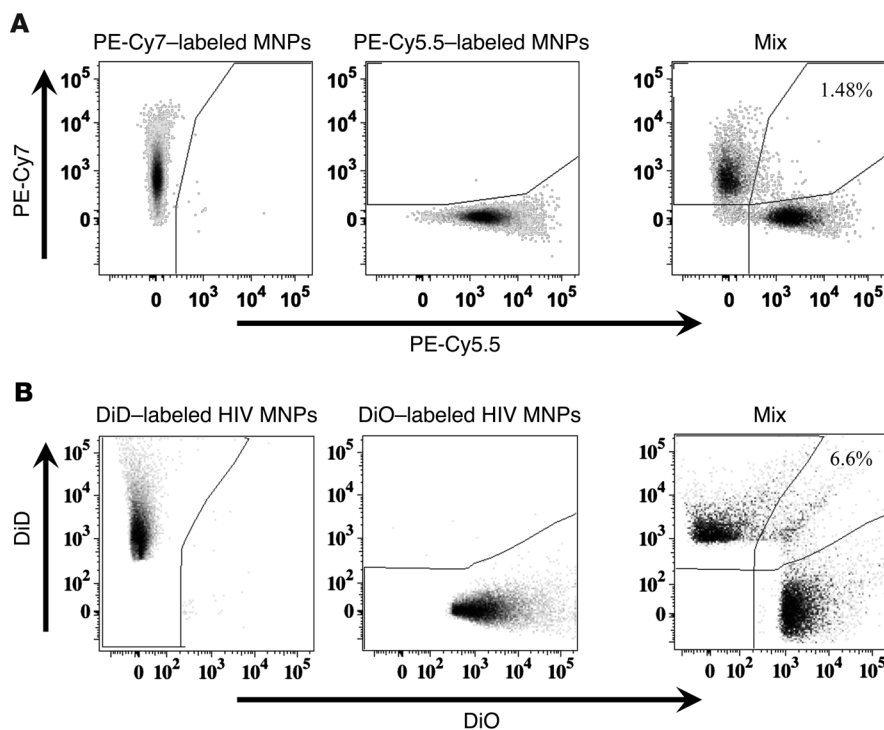
corresponded to single viral particles, we performed a series of control experiments:

First, we performed four different sets of experiments to confirm that the staining of HIV-1-MNP complexes with anti-gp120 anti-

bodies was specific and revealed bound virions: (a) flow analysis showed that in a control preparation from which virus was omitted, only  $0.9\% \pm 0.3\%$  ( $n = 9$ ) of the MNPs were positive for gp120 (Figure 2D); (b) when the entire procedure was performed with the ΔENV-GFP-HIV-1 variant, only  $1.2\% \pm 0.3\%$  ( $n = 4$ ) of the MNPs were positive for GFP (Figure 2E); (c) isotype control staining of HIV-1-MNP complexes with purified Alexa Fluor 647-labeled human IgG1 and eFluor 450-labeled IgG1 κ resulted on average in the positivity of only  $0.28\% \pm 0.06\%$  and  $0.05\% \pm 0.005\%$  ( $n = 3$ ) of events, respectively, confirming the specificity of staining for gp120 (Figure 2F) and CD45 (Figure 2G); (d) when instead of HIV-1, we used a preparation of microvesicles produced by uninfected cells, on average only  $2.05\% \pm 0.28\%$  ( $n = 2$ ) of events negative for CD45 were positive for staining with 2G12, again confirming the specificity of viral capture and detection (Figure 2H). Together, these data confirm that about 90% of the events detected by flow analysis represent captured virions. To focus on HIV-1 virions, we continued to use staining for CD45 in our gating strategy to exclude microvesicles.

Second, we evaluated the fraction of virions captured by anti-gp120-MNP complexes by comparing the amount of HIV in the MNP's captured-fraction with the amount of HIV in the sample prior to capture. Based on RNA quantification, in these two fractions, on average,  $18.1\% \pm 2.7\%$  ( $n = 4$ ) of virions were bound to the VRC01-MNP complexes and were eluted from the column after magnetic separation. We confirmed these results by using GFP-expressing HIV-1 virions, which can be directly visualized by flow cytometry. In this experiment, for the accuracy of viral enumeration, we added AccuCheck beads

to measure the volume of the sample acquired in flow analysis to calculate the concentration of viruses in the samples. The amount of viruses captured by MNPs, as evaluated by GFP measurement, constituted 18.3% of the viruses in the sample before purification.

**Figure 3**

Single particle detection. (A) Two preparations of labeled MNPs, one complexed with PE-Cy7-labeled antibody (left panel) and the other with a PE-Cy5.5-labeled antibody (center panel) were mixed (right panel). Of the events recorded, approximately 1.5% appeared to be double positive (right panel). Thus, approximately 98.5% of events represent single MNPs. Results represent one of four experiments. (B) A preparation of HIV-1<sub>SF162</sub> was divided into two parts: one part was stained with DiD (left panel) and the other with DiO (center panel). The two preparations were mixed, and the virions were captured by MNPs and analyzed (right panel). Note, about 90% of the events represent individual HIV-1 virions. Results represent one of four experiments. On each plot, the fraction of events in their respective gates is expressed as a percentage of the total events in the plot.

To evaluate the percentage of virions that were recognized by VRC01 but not retained by the magnetic columns, we collected the flow-through fraction of virions and captured it once again with VRC01-MNP complexes followed by magnetic purification and flow analysis. We found that 3% of virions not captured in the first run were bound to VRC01-MNPs.

Thus, MNPs complexed with VRC01, an antibody recognizing trimeric gp120, are able to capture 97% of virions that carry the cognate antigen containing the epitope recognized by this capture antibody. To characterize further virions that were not recognized by the VRC01-MNPs and thus not retained by the magnetic column, we recaptured them with the 2G12-MNPs and subjected them again to magnetic column separation. On average,  $42\% \pm 14\%$  ( $n = 3$ ) of those virions were recaptured. Thus, the virions in the stock that were not recognized by the VRC01-MNPs were either defective and did not express gp120, or expressed gp120 in a conformation that was not recognized by this broadly neutralizing antibody.

Third, we evaluated the infectivity of the viral preparation that was not captured by the VRC01-MNP complexes. Toward this goal, we estimated the TCID<sub>50</sub> of this viral suspension using TZM-bl cells. For HIV-1<sub>SF162</sub> and HIV-1<sub>LAL04</sub>, the infectivities of the applied suspensions were  $7 \times 10^4$  and  $1.5 \times 10^5$ , respectively, while the respective infectivities of the noncaptured viruses were  $8 \times 10^3$  and  $1.4 \times 10^4$ . Thus, the viruses that were not captured by MNPs were approximately 36 times less infectious than the input virus. (Control experiments showed that incubation with noncapturing MNPs and passage through the magnetic column did not change viral infectivity. Data not shown.)

Finally, we investigated whether the events representing HIV-1 bound to anti-gp120 MNPs represent single virions. This was not evident a priori; indeed, two or more MNPs can cross the laser beam simultaneously and be acquired as one event, a phenomenon referred to as “swarm detection” (20). Also, viruses could aggregate

in the course of their binding to MNPs (e.g., by being cross-linked through MNPs or antibodies), again resulting in one event representing many virions. To prove that this was not the case and to estimate swarm detection, we first tested the acquisition coincidence for MNPs themselves. We prepared MNP-antibody complexes labeled with either PE-Cy5.5 or PE-Cy7. When the mixture of these two complexes was subjected to flow analysis, less than 1.5% of events were double positive for both fluorochromes (Figure 3A).

To evaluate which fraction of the events corresponds to single virions, we divided a preparation of HIV-1 into two parts: one was stained with the lipophilic fluorescent green dye DiO and the other with the lipophilic red dye DiD. Then, we mixed these two preparations and bound the virions to MNPs through their anti-gp120 capture antibodies. If the binding of MNPs to viruses resulted in their cross-linking and therefore in the formation of aggregates, then these complexes could be seen as events positive for both fluorochromes. Flow analysis showed that, on average,  $5.04\% \pm 1.21\%$  ( $n = 4$ ) of events were double positive (Figure 3B). These results were confirmed by staining one part of the viral preparation with Pacific Orange and the other with Alexa Fluor 350. Flow analysis of the captured viral mixture showed that about 4% of MNPs were double positive. Thus, in our analysis, about 90% of events represent individual HIV-1 virions.

*Distribution of cellular antigens on HIV-1 virions.* Earlier, it was shown by bulk analysis of HIV-1 preparations that virions contain select cellular antigens acquired by the virus in the process of budding from the cell surface (21). Among the most common are LFA-1 and HLA-DR. We tested whether our technique reveals these particular antigens on virions by staining HIV-1-MNP complexes with anti-LFA-1 and anti-HLA-DR antibodies. The specificity of the staining was verified by incubating HIV-1-MNP complexes with isotype controls. We found that staining with a PE-Cy7-labeled mouse IgG1  $\kappa$  and PE-Cy5.5-labeled IgG2a  $\kappa$ , and isotype controls for LFA-1 and

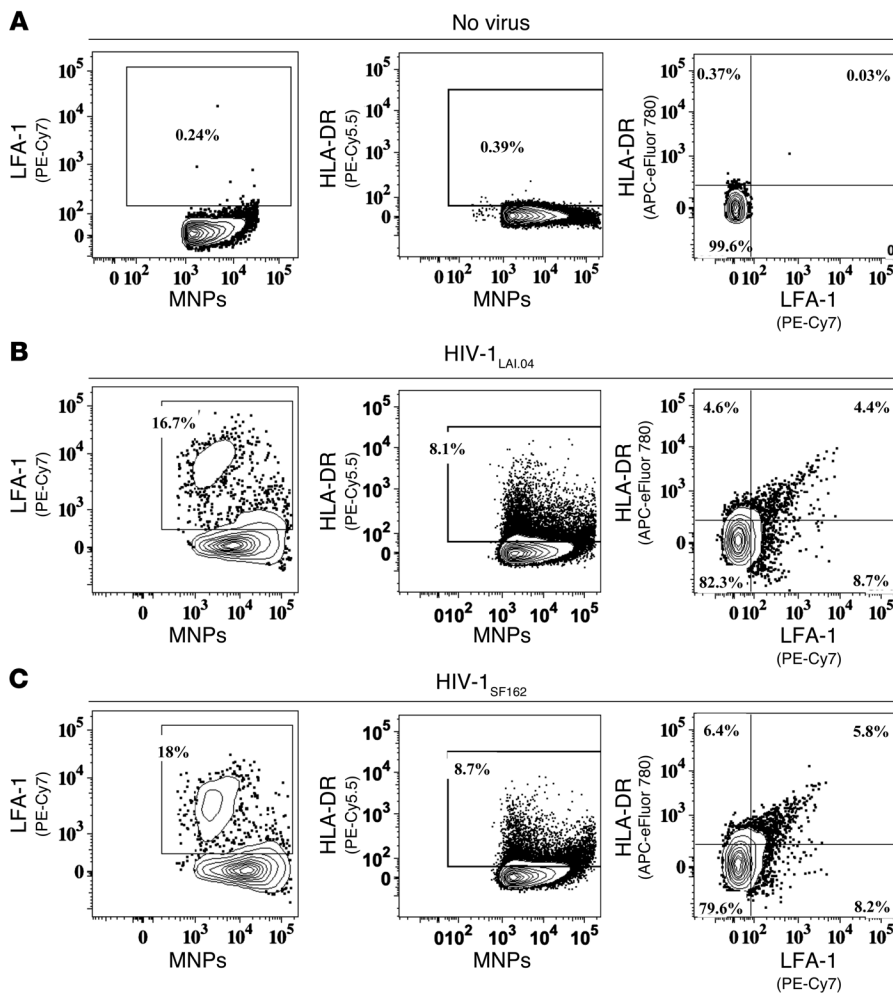


**Figure 4**

Distribution of cellular antigens on HIV-1 virions. HIV-1<sub>LAI.04</sub> and HIV-1<sub>SF162</sub> produced by PBMCs was captured by 2G12-MNPs and visualized with labeled VRC01. (A–C) Following capture, the two cellular antigens were revealed on HIV virions with labeled monoclonal antibodies against LFA-1 and HLA-DR. (A) 2G12-MNPs were incubated with virus-free culture medium and stained with anti-LFA-1-specific antibodies (left panel), anti-HLA-DR-specific antibodies (center panel), or costained for LFA-1 and HLA-DR (right panel). Plots show the positions of the gates used in the gating strategy shown in Figure 2A. Note the low nonspecific binding of antibodies to 2G12-MNPs. (B and C) Staining of HIV-1<sub>LAI.04</sub>-2G12-MNP complexes (B) and HIV-1<sub>SF162</sub>-2G12-MNP complexes (C) for LFA-1 (left panels), HLA-DR (center panels), or costaining for both antigens (right panels). Note the heterogeneity of the viral preparation regarding these two cellular antigens. Representative experiments of three to six replicate experiments.

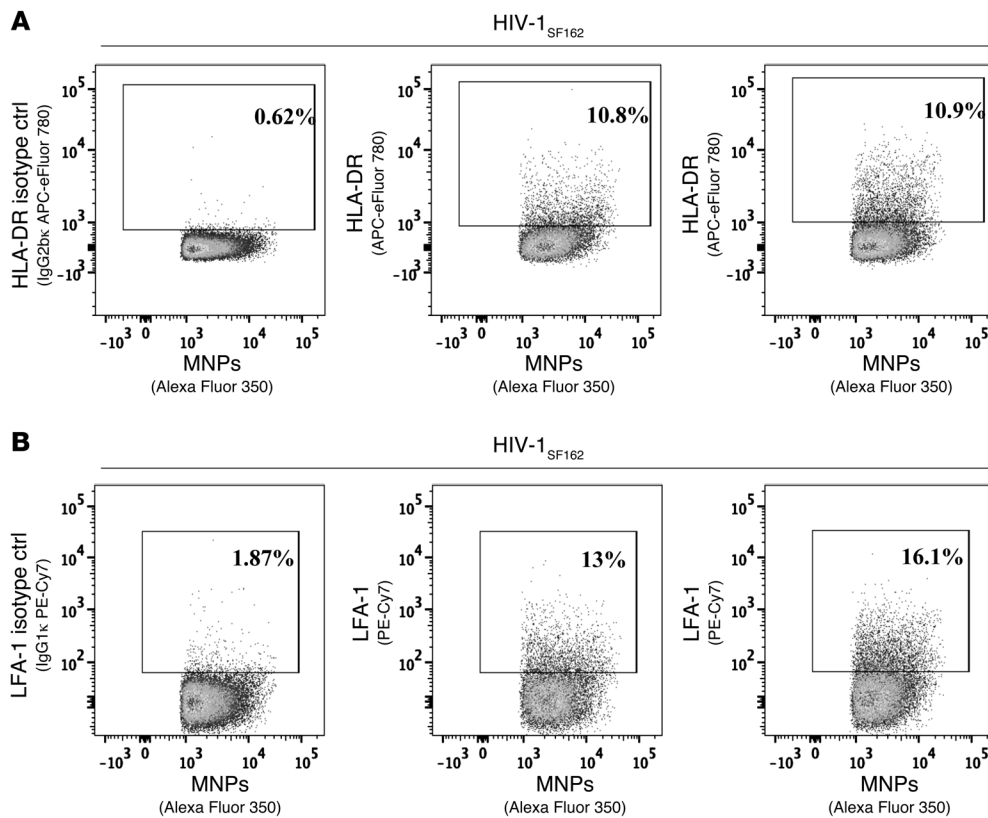
HLA-DR, respectively, resulted on average in  $0.17\% \pm 0.04\%$  and  $0.87\% \pm 0.02\%$  ( $n = 3$ ) positive events (Figure 4A). In addition, we confirmed the specificity of staining by performing the entire staining procedure in the absence of HIV-1 virions (Figure 4A).

Unlike techniques reported earlier, flow virometry allows not only the demonstration of the presence of these antigens on viruses but, importantly, the analysis of the distribution of antigens among individual viral particles. Here, we evaluated the distribution of HLA-DR and LFA-1 on two HIV-1 variants replicated in two different cell preparations.

We analyzed the presence of LFA-1 and HLA-DR on individual virions of HIV-1<sub>LAI.04</sub> and HIV-1<sub>SF162</sub> produced in PBMCs. HIV-1 was bound to MNPs via VRC01 capture antibody against gp120. As described above, we confirmed viral binding by labeling these complexes with another anti-gp120 antibody, 2G12. Cellular antigens were detected on MNP-immobilized virions, with antibodies against LFA-1 and HLA-DR labeled with different fluorochromes. Flow virometry showed that LFA-1 and HLA-DR were present, on average, on  $16.7\% \pm 2.0\%$  ( $n = 6$ ) and  $8.6\% \pm 0.3\%$  ( $n = 3$ ) of HIV-1<sub>LAI.04</sub> virions, respectively, while  $4.8\% \pm 0.6\%$  ( $n = 3$ ) of all virions carried both antigens (Figure 4B). Flow virometry of HIV-1<sub>SF162</sub> produced in PBMCs revealed the presence of these antigens on  $20.0\% \pm 4.4\%$  ( $n = 6$ ) and  $10.8\% \pm 1.3\%$  ( $n = 6$ ) of virions, respectively, whereas  $6.55\% \pm 0.4\%$  of virions were double positive (Figure 4C).

To prove that it is not because MNPs block access of the antibodies to HLA-DR and LFA-1 that the latter virions appear negative for these antigens, we first evaluated the amount of MNPs bound to the virions of each phenotype. In contrast to what would be expected if the MNPs blocked access of anti-LFA-1 or anti-HLA-DR to their respective antigens, the MFI of specific MNPs on virions positive for HLA-DR, LFA-1, or for both cellular antigens was not lower than the MFI of MNPs on virions that were double negative for both markers and actually was, on average,  $7.0 \pm 1.4$  times higher ( $n = 12$ ,  $P = 0.001$ ). Second, to confirm that MNPs do not block access of anti-HLA-DR and anti-LFA-1 antibodies, we first incubated the viral suspension with these antibodies and then with capture VRC01-MNPs. This reversion did not significantly change ( $P > 0.1$ ) the distribution of the virions according to the two cellular antigens LFA-1 and HLA-DR, which were present on  $14.8\% \pm 0.6\%$  ( $n = 7$ ) and  $13.2\% \pm 0.9\%$  ( $n = 7$ ) of virions, respectively (Figure 4, D and E), whereas  $8.7\% \pm 0.4\%$  of virions were double positive. Thus, MNPs do not block binding of HLA-DR and LFA-1 antibodies to viral surfaces, and the HIV-1 virions of the same preparation are indeed antigenically heterogeneous.

Next, we compared the distributions of LFA-1 and HLA-DR among HIV-1<sub>LAI.04</sub> and HIV-1<sub>SF162</sub> virions produced in PBMCs, presented above, with those among the same viruses produced in Jurkat cells. The two cellular antigens were present on  $1.6\% \pm 1.4\%$  ( $n = 3$ )

**Figure 5**

MNP binding and accessibility of cellular antigens on virions. HIV-1<sub>SF162</sub> was produced by PBMCs, captured on MNPs via anti-gp120 antibody VRC01, visualized with labeled 2G12 antibodies, and stained for two cellular antigens with anti-HLA-DR and anti-LFA-1 antibodies. Alternatively, the same preparation of HIV-1<sub>SF162</sub> virions was first incubated with anti-LFA-1 and anti-HLA-DR antibodies and then captured on VRC01-MNPs and visualized with 2G12 antibodies. (A) HLA-DR, (B) LFA-1. Left panels: isotype controls. Center panels: staining of MNP-captured virions for HLA-DR and LFA-1. Right panels: staining of virions for HLA-DR and LFA-1 followed by capture with MNPs. Note that the reverse order of staining for cellular antigens and capture with VRC01-MNPs did not significantly affect the result (see the text for the statistical analysis). Results represent one of seven experiments. On each plot, the fraction of events in their respective gates is expressed as a percentage of the total events in the plot.

and  $1.6 \pm 0.7\%$  ( $n = 4$ ) of HIV-1<sub>LAI.04</sub> virions and on  $7.2 \pm 2.5\%$  ( $n = 3$ ) and  $5.6 \pm 2.7\%$  of ( $n = 4$ ) of HIV-1<sub>SF162</sub> virions produced in Jurkat cells, respectively (Figure 5). The low expression of both antigens on Jurkat cell-produced viruses, which prevented us from reliably evaluating the fraction of virions coexpressing both antigens, reflects the low expression of these antigens by Jurkat cells themselves (data not shown). Thus, for the same HIV-1<sub>LAI.04</sub> variant, which was produced in two different cells, the antigenic makeup of the virions becomes different, at least for HLA-DR ( $P < 0.01$ ) and LFA-1 ( $P < 0.02$ ). A similar tendency was observed with HIV-1<sub>SF162</sub>, but in this case it did not reach statistical significance.

Finally, the data presented above allowed us to compare the distributions of LFA-1 and HLA-DR in two different HIV-1 preparations, HIV-1<sub>SF162</sub> and HIV-1<sub>LAI.04</sub>, produced in the same cells, either PBMCs or Jurkat cells. These data (Figure 6) show that, although the fractions of LFA-1- and HLA-DR-containing HIV-1<sub>SF162</sub> and HIV-1<sub>LAI.04</sub> virions produced in PBMCs are different, the ratios of these fractions are similar ( $P > 0.21$ ). The same is true for HIV-1<sub>SF162</sub> and HIV-1<sub>LAI.04</sub> virions produced in Jurkat cells ( $P > 0.21$ ). Thus, at least for the two cellular antigens evaluated here, the antigenic

makeup of two different HIV-1 preparations produced in the same cells became somewhat similar.

*Flow analysis of virions in bodily fluids.* We evaluated whether flow analysis of HIV-1 virions can be directly performed in the context of bodily fluids. Toward this goal, we first reproduced the capture protocol developed for PBS-suspended virus, except that virus (HIV-1<sub>NL4.3</sub>) was suspended in normal blood plasma. HIV-1 virions bound to VRC01-MNPs were revealed by flow virometry with labeled 2G12 antibodies. After capture of virus with VRC01-MNPs and separation on a magnetic column, on average,  $87.7\% \pm 2.6\%$  ( $n = 4$ ) of VRC01-MNPs were labeled with anti-gp120 antibodies, similar to what is observed in virus suspended in PBS. Also, similarly to virus suspended in PBS, 17.8% of virions suspended in plasma were captured by VRC01-MNPs and retained by the column as evaluated by enumerating GFP-HIV-1 virions.

Similarly, we were able to visualize virions in cervicovaginal lavage (CVL) spiked with HIV-1<sub>NL4.3</sub>. In this case, on average,  $58.8\% \pm 3.8\%$  ( $n = 3$ ) of VRC01-MNPs were labeled with anti-gp120 2G12 antibodies. In these experiments,

the capture efficiency was  $18.2\% \pm 5.8\%$  ( $n = 3$ ).

However, in patients' plasma, the amount of virus was much lower than in the above-described model experiments ( $1.1 \times 10^4$  to  $1.6 \times 10^5$  copies per milliliter, an order of magnitude lower than that in our model experiments). Therefore, we modified our protocol to first concentrate virus using an additional magnetic concentration step. Specifically, we used 4 ml of plasma (rather than the 60  $\mu$ l used in the case of viral stock) and first concentrated plasma virions by capturing them on the VRC01-MNP complexes followed by separation on magnetic columns. The retained virus-MNP complexes were eluted, stained with the 2G12 detection antibody, and again separated on a magnetic column as described in Methods. This protocol was first used in a simulated experiment when normal plasma was spiked with HIV-1<sub>SF162</sub> at a concentration similar to that of the virus in patients' plasma. In this case, the amount of beads in the final preparation was several-fold larger, and thus the fraction of beads that carried virions was lower than that in our initial protocol. Nevertheless, we could reliably visualize viral particles captured by VRC01-MNPs and detected by 2G12, and as was the case in the control experiments

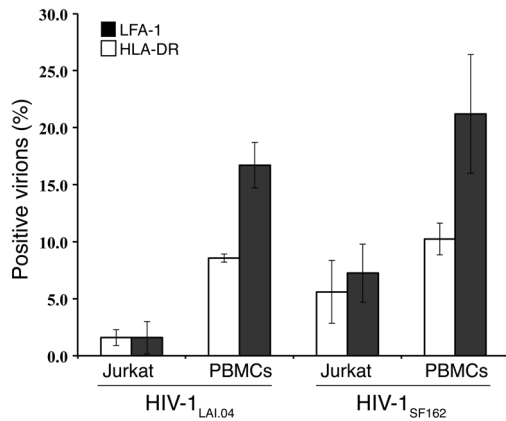


**Figure 6** Distribution of cellular antigens on HIV-1<sub>LAI.04</sub> and HIV-1<sub>SF162</sub> produced in two different cell types. HIV-1<sub>LAI.04</sub> and HIV-1<sub>SF162</sub> were produced either in PBMCs or in Jurkat cells. Preparations of HIV-1 were captured on MNPs via VRC01, and virions were visualized with Alexa Fluor 647–labeled 2G12. The presence of HLA-DR (white bars) and LFA-1 (black bars) were revealed with PE-Cy5.5– and PE-Cy7–labeled antibodies specific to these antigens, respectively. Presented are the averages ± SEM of three to six experiments.

with virus-free plasma or with the isotype antibodies, the number of positive events was below 0.9% (Figure 7A).

Finally, we applied flow virometry to blood plasma that was derived from HIV-infected individuals (Figure 7B). The recovery of plasma virions by VRC01-MNPs, as evaluated by RNA concentration using RT-PCR, was again about 16% and was not significantly different from the recovery measured in the above-described experiments with laboratory-produced viruses suspended either in PBS or in normal blood plasma or CVL.

Finally, as a proof of concept, we verified that it was possible to perform the analysis of the distribution of the two cellular antigens LFA-1 and HLA-DR on patient-derived viruses (Figure 7, C and D). In a plasma sample from an HIV-1–infected individual, 12.4% of captured virions carried LFA-1, 41.8% carried HLA-DR, and 9.5% carried both antigens.

Thus, flow virometry can be applied to characterize the antigenic makeup of HIV-1 in bodily fluids.

## Discussion

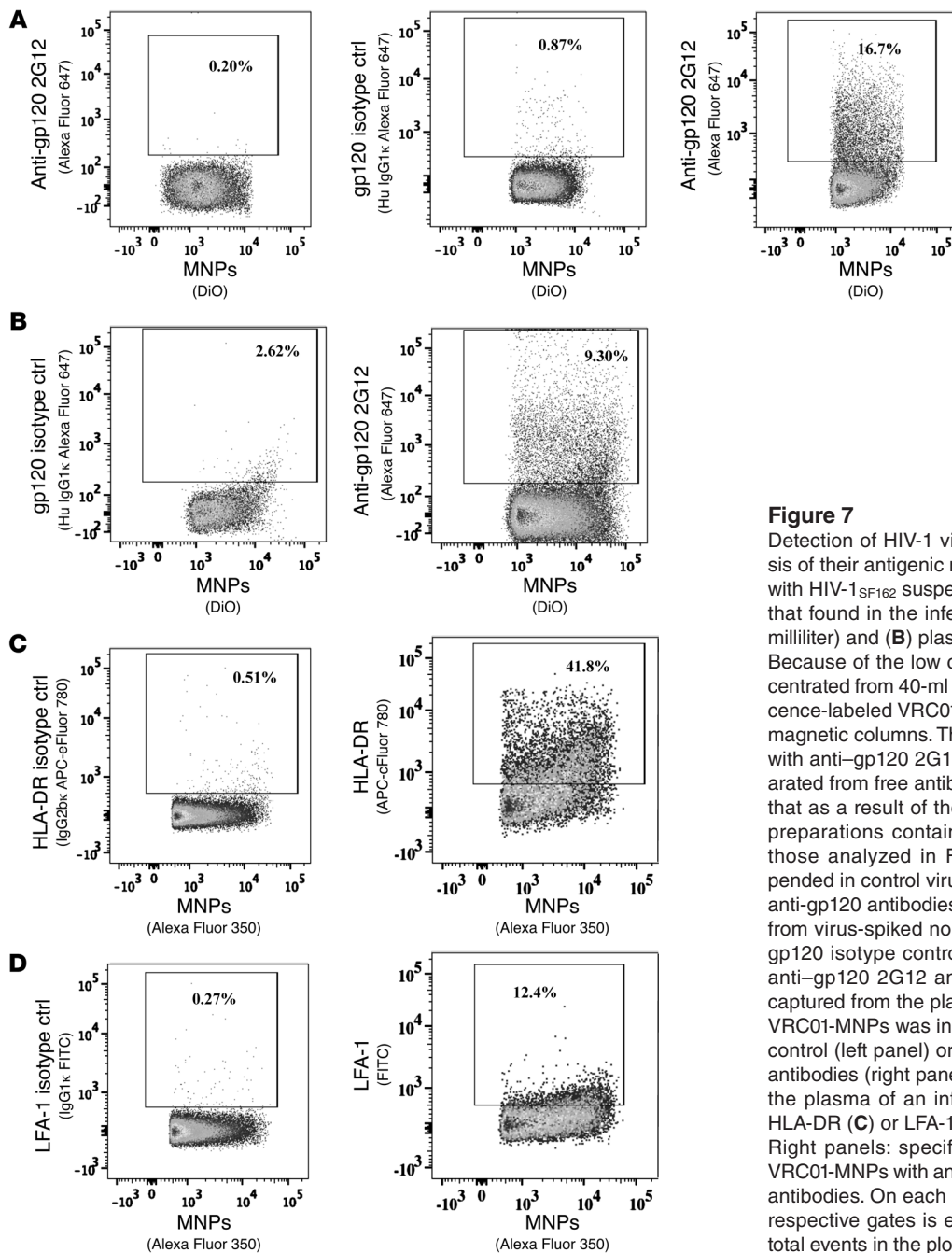
In this work, we describe a new technology, flow virometry, which we believe allows for the first time the evaluation of the antigenic variability of individual viral particles.

HIV-1 antigenic variability stems not only from the high mutagenicity of its genome, but also from the virus' ability to include various cellular molecules that may significantly alter viral properties. Up to now, the presence of these proteins has been studied in viral preparations either with ELISA or with flow cytometry of multiple viruses bound to microbeads (9, 12, 22–27). These studies analyzed viral particles in bulk. Individual viral particles labeled with fluorescent dyes have been observed in microscopic imaging studies (28) that addressed HIV-1 assembly (29–31) and infection (32, 33), particularly in transmission to the female lower genital tract (34), however, they did not characterize these particles antigenically. Immunoelectron microscopy has identified several anti-

gens on viral particles (35), but few virions can be analyzed with this laborious technique.

Flow virometry, described here, allows for easy identification and analysis of multiple antigens on a virtually unlimited number of individual viruses. Briefly, the technique we developed consists of four major steps: (a) Immobilization of virions onto 15-nm MNPs coupled with capture antiviral antibodies. In this work, we used antibodies against gp120, a ubiquitous HIV-1 protein (36). (b) Labeling of nanoparticle-immobilized HIV-1 with a set of fluorescence-labeled monoclonal antibodies that reveal antigens on the virions. In this work, we focused on two cellular antigens that the virus acquires from the infected cells, however, our technology can be used to analyze any viral surface antigen, provided that a specific fluorescent probe is available. (c) Separation of the nanoparticle-immobilized virus from unbound antibodies. Magnetic properties of the nanoparticles allow the separation of the immobilized virus on magnetic columns. (d) Nanoparticle-immobilized viruses retained on the magnetic column and then eluted are subjected to flow analysis using a conventional flow cytometer with a modified setting. Routinely, in flow cytometers, a cell that passes through the laser beam and scatters light constitutes an event that triggers the recording of the fluorescent spectra emitted by cell-bound fluorescent antibodies. In flow virometry, nanoparticles themselves are labeled with a fluorescent Fab against the Fc portion of the capture antibody that is coupled to them. In this way, nanoparticle-immobilized viruses trigger the flow cytometer with their fluorescence, as they are too small to generate a light-scatter event. Indeed, fluorescence detection of submicroscopic particles is less susceptible to artifacts than light scattering (37), which is often the result of swarm detection (20). The lack of detection of double-positive events in experiments, in which beads or viruses individually stained with either of two fluorochromes are mixed, argues against swarm detection under our experimental conditions.

To confirm that the protocol described above results in HIV-1 virion immobilization on nanoparticles, we analyzed the nanoparticles for the presence of an HIV-1 hallmark molecule, gp120. We used an anti-gp120 antibody that recognizes an epitope different from the one recognized by the capture antibody. In the present work, we alternatively used two anti-gp120 antibodies, VRC01 and 2G12, one for capture and the other for detection. Without HIV-1, almost no nanoparticles were positive for gp120. Also, by staining with isotype control antibodies and using a preparation of microvesicles instead of virions, we were able to demonstrate the specificity of viral identification. These experiments show that not only unbound fluorochrome-labeled antibodies, but also free fluorochromes, which contaminate most labeled antibody reagents, are removed prior to flow acquisition. Moreover, these contaminants cannot compromise our technique, since HIV virions are recognized by colocalization of fluorescent antibodies against the capture anti-gp120 antibody of the MNP complexes and antibodies targeting gp120 on the virions, and by the fluorescence from antibodies targeting viral antigens of interest. Also, viruses purified on MNPs were not markedly contaminated by microvesicles, as about 99% the viral particles we captured did not carry CD45, an antigen that distinguishes them from cellular microvesicles (18), while microvesicles expressing CD45 were readily identified in the same viral preparation. In our gating strategy, we excluded CD45-positive microvesicles, and the remaining 1% may represent microvesicles that carry gp120.

**Figure 7**

Detection of HIV-1 virions in blood plasma and analysis of their antigenic makeup. Normal blood plasma (A) with HIV-1<sub>SF162</sub> suspended at a concentration similar to that found in the infected donors ( $10^4$ – $10^5$  copies per milliliter) and (B) plasma from an HIV-1-infected donor. Because of the low concentration, virus was first concentrated from 40-ml samples by capturing it on fluorescence-labeled VRC01-MNPs followed by separation on magnetic columns. Then, captured virions were stained with anti-gp120 2G12 antibodies and once again separated from free antibodies on magnetic columns. Note that as a result of the concentration procedure, these preparations contain substantially more MNPs than those analyzed in Figure 2. (A) VRC01-MNPs suspended in control virus-free plasma and incubated with anti-gp120 antibodies (left panel); MNP-captured HIV-1 from virus-spiked normal plasma incubated with anti-gp120 isotype control antibody (center panel) or with anti-gp120 2G12 antibodies (right panel). (B) HIV-1 captured from the plasma of an infected individual with VRC01-MNPs was incubated with either gp120 isotype control (left panel) or visualized with anti-gp120 2G12 antibodies (right panel). (C and D) HIV-1 captured from the plasma of an infected individual was stained for HLA-DR (C) or LFA-1 (D). Left panels: isotype controls. Right panels: specific staining of HIV-1 captured by VRC01-MNPs with anti-HLA-DR (C) and anti-LFA-1 (D) antibodies. On each plot, the fraction of events in their respective gates is expressed as a percentage of the total events in the plot.

The entire identification of HIV-1 virions is based on their recognition by MNPs that carry capture (anti-gp120) antibodies. No MNP-bound virions were revealed when  $\Delta$ ENV viral preparations were subjected to flow virometry. However, not all HIV-1 virions with ENV were bound to MNPs via anti-gp120 and thus retained by magnetic columns. It seems that VRC01-MNPs capture about 20% of virions in the viral stock. To check whether the remaining 80% of virions are just “lost” due to the inefficiency of our technique or whether they are not recognized by VRC01, we collected virions that were not retained by the magnetic column and subjected them once again to the entire procedure of recapture by VRC01-MNPs and magnetic separa-

tion. These experiments showed that only 3% of the virions not bound by VRC01-MNPs, and thus not retained by the magnetic column in the first run, were recaptured. However, about 40% of these virions, which are not recognized by the VRC01-MNPs, can be captured with 2G12-MNPs.

Thus, our technique analyzes about 95% of virions that carry gp120 trimers recognizable by the capture VRC01 coupled to the MNPs. Moreover, those virions that are not captured by the VRC01-MNPs seem not only to be antigenically different, but are also 36-fold less infectious, which may in part be due to the improper conformation of their ENV, which render it incapable of being recognized by VRC01. The lower infectivity of the virions





that are not recognized by VRC01-MNPs is in general agreement with the ability of VRC01 to broadly neutralize HIV.

In summary, our technique efficiently analyzes virions that are recognized by particular anti-gp120 antibodies. Using different anti-gp120 antibodies, it would be possible to probe the ENV conformation on individual viral particles. In general, these data are in agreement with a bulk analysis of anti-gp120 antibodies binding to HIV-1 that showed that VRC01 antibodies recognize about 20% of virions (R.J. Shattock, personal communication). The differential virion capture by MNPs bound to particular anti-ENV antibodies reflects the antigenic composition of this virus, and the amount of the captured virions seems to reflect the size of the fraction carrying that particular antigen. Indeed, when the above-described protocol was applied to fluorescently labeled dengue virions, all of which carry the E protein antigen (38), MNPs coupled to the anti-E protein antibody 3H5 (39) captured close to 95% of viruses (Supplemental Figure 2). In general, our results are in agreement with the notion that a significant fraction of virions generated *in vitro* and *in vivo* are defective. The inability of virions to be recognized by VRC01 antibodies may be one of the manifestations of these defects. The nature of these defects on individual viral particles can now be analyzed using MNPs that carry antibodies recognizing different epitopes on ENV.

To characterize virions that bind anti-gp120-MNP complexes, it is important that each fluorescent event represent one virion, rather than viral aggregates formed due to the anti-gp120-MNPs cross-linking or to the binding of two or more virions to the same nanoparticle. Also, to resolve individual virus-MNP complexes, they should not simultaneously enter the laser beam of the flow cytometer. Several control experiments showed that about 90% of events represent individual viral particles whose antigenic makeup can now be characterized.

The technique we developed should be used not only to analyze laboratory HIV-1 stocks, but could also be applied to bodily fluids of HIV-1-infected individuals. To this end, we first spiked normal CVLs and blood plasma with HIV-1 and found that the protocol we developed does not depend on whether HIV-1 is suspended in PBS or in one of these bodily fluids. Finally, we subjected blood plasma from HIV-1-infected individuals to flow cytometry. Although the viral load for some patients may reach values close to those we used for experiments with laboratory HIV-1 strains, the loads in clinical samples were typically lower. Therefore, for this analysis we slightly adapted our techniques by first concentrating the viruses from a large sample volume. This was done by binding virions to MNPs through the capture antibody, followed by separating the bound virions on magnetic columns and eluting the bound fraction into a small volume. This resulted in a higher concentration of MNPs compared with that obtained under our original protocol. We were now able to analyze this concentrated preparation with flow virometry, similarly to the analysis of laboratory strains of HIV-1 suspended in PBS. Because of the higher concentration of beads, the fraction of MNPs that captured virus was accordingly reduced in the bodily fluid analysis. However, the efficiency of viral capture by VRC01-MNPs did not seem to be changed and constituted around 20% of the viruses. Also, various factors in bodily fluids may have interfered with HIV binding to MNPs or may have increased the frequency of MNP aggregates that were excluded from the analysis by the gating strategy. This may explain the difference we found in the fractions of MNPs that bound viruses in blood plasma and CVLs.

Thus, flow virometry can be applied both as a tool for analysis of individual viruses in the laboratory setting and in the clinical setting for analysis of samples obtained directly from HIV-1-infected patients. Direct analysis of patients' viruses seems to be more effective than some of the commonly used techniques that first require the propagation of patients' isolates in cell culture, which may change the properties of these isolates.

Although all the viruses carry gp120 on their surface, they are heterogeneous in terms of the cellular antigens they carry. Already, the results of the first experiments with our new technology demonstrate its advantage over existing technologies. Indeed, two cellular antigens that were earlier reported to be associated with HIV-1 preparations (16, 17, 40) (and which because of this were chosen for the current analysis), HLA-DR and LFA-1, were not present on individual virions and were not equally distributed among them. Some viral particles carry one of these two antigens, while others carry both. This diversity is not explained by steric hindrance caused by bound MNPs, as staining virions for these antigens followed by MNP capture did not change the distribution of these antigen-carrying virions. Also, the amount of bound MNPs on virions that were double negative for these cellular antigens was even smaller than the amount of MNPs bound on virions that were positive for these antigens. The latter may be explained by colocalization of ENV and cellular antigens on the viral surface. In these experiments, we used viral suspension from which free gp120 had been removed by centrifugation (see Methods). Otherwise, some of the LFA-1/HLA-DR double-negative events could be attributed to free gp120 molecules captured by anti-gp120 MNPs and detected by another anti-gp120 antibody. In the case of patient-derived plasma, gp120 was not removed, but the majority of events were HLA-DR positive and thus could not represent binding of free gp120 molecules.

In our experiments, the antigenic makeup is determined both by the HIV-1 genotype and by the cells from which the virus originates, and the latter determinant seems to predominate. In the case of PBMCs, the presence of the small number of monocytes/macrophages may affect the distribution of virions according to the cellular proteins. Different virions of a single HIV-1 variant originating from cells of two different types have different spectra of two cellular antigens, whereas two genotypically different viruses (one using CCR5 and another CXCR4 as a coreceptor) but originating from the same cells become similar in their cellular antigenic composition. While it is in agreement with the earlier reported bulk analysis of viral preparations that revealed these antigens (4, 21–24, 41, 42), flow virometry allows the comparison of the distributions of particular antigens on virions produced by different cells. Further studies using flow virometry will show the biological role of cellular antigens presented on HIV-1 virions. Moreover, the analysis of HIV-1 produced by lymphoid tissue *ex vivo* revealed that the distribution of HLA-DR on virions changes in the course of infection (data not shown), probably reflecting the HIV-1-triggered upregulation of this activation marker on infected and bystander T cells (43).

Although the technique we developed has the advantage of addressing the characteristics of individual virions one at a time, it has its own limitations.

Here, in our experiments, of five colors used, only three were dedicated to analyzing cellular antigens carried by HIV-1 virions. With contemporary flow cytometers, up to eighteen colors can potentially be used to identify antigens on viruses in a single



flow analysis. However, while we did not find evidence of steric hindrance between MNPs and the two cellular antigens revealed here, steric hindrance may restrict the number of antigens simultaneously identified on a single virion. Irrespective of the number of identifiable markers, in the next steps of the development of this technology, virus-MNP complexes could be sorted and subjected to modern virological and molecular biological assays. Although sorting of virions itself does not seem to be a problem, whether virions bound to MNPs retain their infectivity and, if so, it remains to be addressed whether they infect cells via binding to receptors and coreceptors and via fusion. Finally, the presence of endogenous antibodies against HIV antigens in patients' blood may interfere with virion capture and analysis and makes the choice of the capture antibody difficult. Future studies may reveal other limitations of flow virometry.

Whatever these limitations are, the new method described here constitutes a technical advance that will help address the question of viral infectivity and transmissibility at the level of a single viral particle and thus may provide new insights into the basic mechanisms of viral infection and lead to the development of new more precisely targeted antivirals. For example, with the new technique, it may be possible to characterize the antigenic makeup of HIV-1 variants that transmit infection (the transmitted/founder HIV-1 variants). Further characterization of cellular antigens carried by the virions may allow them to be traced to the particular cells and tissue in which they replicated (44) and to determine which cells contribute to viral load at different stages of HIV-1 disease. Finally, we think that with our technique, it will be possible to study viral association with antibodies generated in an infected individual independently of their ability to neutralize these viruses.

## Methods

**Virus preparations.** CXCR4-tropic LAI.04 (HIV-1<sub>LAI.04</sub>) or CCR5-tropic SF162 (HIV<sub>SF162</sub>) (82 ng/ml,  $2.9 \times 10^8$  RNA copies/ml and 37.8 ng/ml,  $4.74 \times 10^8$  RNA copies/ml, respectively) were produced in phytohemagglutinin-P-stimulated (PHA-P-stimulated) PBMCs by the VQA (Rush Medical School, Chicago, Illinois, USA) using the AIDS Clinical Trials Group's (ACTG) standard operating procedure. A second pair of these viruses was obtained by infection of Jurkat-tat-2H5 cells (gift of Q. Sattentau, Dunn School of Pathology, University of Oxford, Oxford, United Kingdom). These cells were grown in RPMI supplemented with 10% FCS, 50 µg/ml gentamycin, 0.5 µg/ml hygromycin, and 0.5 mg/ml G418. Cells ( $10^6$ ) were inoculated with 100 µl of either of the two HIV-1 variants at 37°C. Viral infection was monitored by flow cytometry of cells stained for intracellular p24 with the PE-labeled anti-p24 Ab KC57 (Beckman Coulter). When 40% of cells became p24 positive,  $5 \times 10^6$  cells were added. Twenty-four hours later, the cells were centrifuged (500 g for 10 minutes) and supernatant containing virus was collected. All obtained viral stocks were quantified for their p24 GAG content, diluted to a concentration of 2.59 µg/ml, and frozen in 60-µl aliquots at -80°C. In experiments aimed at analyzing the specificity of HIV-1 capture and staining, we used preparations of microvesicles derived from the SUPT1-CCR5 CL.30 cell line that were purified on sucrose gradients and diluted 1:10 from a stock at a concentration of 1.03 mg/ml. The GFP-expressing HIV-1<sub>NL4-3</sub> variant was provided by T. Hope (Northwestern University, Chicago, Illinois, USA). The stock of this virus contained  $4.8 \times 10^9$  virions per milliliter. HIV-1<sub>NL4-3</sub>, provided by J. Lifson (SAIC-Frederick, NCI Frederick, Frederick, Maryland, USA), was produced in SUPT1-CCR5 cells and was purified by ultracentrifugation on a density gradient, separating the viral stock from cellular debris and protein aggregates, including gp120.

**Coupling of monoclonal antibodies to magnetic nanoparticles.** One milligram of 15-nm carboxyl-terminated magnetic iron oxide nanoparticles (Ocean NanoTech) was coupled to human monoclonal antibodies against HIV-1 gp120, either VRC01 (gift of J. Mascola, VRC, NIH, Bethesda, Maryland, USA) or 2G12. Briefly, 1 mg of MNPs was incubated in 400 µl of activation buffer supplemented with 1.7 mM 1-(3-dimethylaminopropyl)-3-ethylcarbodiimide hydrochloride (EDAC) and 0.76 mM N-hydroxysulfosuccinimide (sulfo-NHS) for 20 minutes at room temperature. After activation, 500 µl of coupling buffer was added to the particles, immediately followed by the addition of 1 mg of the purified antibody. After 2-hour coupling in a thermomixer at room temperature with gentle mixing, the reaction was stopped by adding 10 µl of quenching solution and transferred to a 12 × 75 mm tube. Two wash steps with wash/storage buffer were performed using a SuperMAG-01 magnetic separator (Ocean NanoTech) at 4°C. The coupled MNPs were suspended in 4 ml of storage buffer and stored at 4°C at an iron oxide concentration of 0.25 mg/ml.

**Capture and detection of HIV with nanoparticles.** HIV-1 viral stocks (60 µl; between  $1.14 \times 10^7$  and  $2.47 \times 10^7$  virions, based on the p24 content) were incubated with 60 µl ( $3.9 \times 10^{12}$ ) of anti-gp120-coupled MNPs for 40 minutes at 37°C with continuous mixing. Host cell proteins incorporated into viruses were revealed with a mixture of monoclonal antibodies. In our experiments, we used 3 µl each of the following monoclonal antibodies: anti-HLA-DR PE-Cy5.5 (or anti-HLA-DR APC-eFluor 780), anti-LFA-1 PE-Cy7, anti-CD45 eFluor 450 (eBioscience), and 3 µg of VRC01 labeled in-house with Alexa Fluor 647 (Invitrogen, Life Technologies), or their matched isotype controls. Also, we performed staining control, in which one antigen-specific antibody at a time was omitted from the staining (fluorescence minus one controls) (Supplemental Figure 3). The mixtures were incubated at room temperature for 15 minutes.

In order to visualize the MNP-VRC01 complexes, 4 µg of an Alexa Fluor 488-labeled goat anti-human IgG Fab (Jackson ImmunoResearch) was then added to the mixture and incubated for 5 minutes at room temperature. The HIV-1-MNP complexes with bound antibodies were separated from unbound reactants on µMACS magnetic columns mounted on a high-field µMACs magnet (both from Miltenyi Biotec). The columns were washed three times with the washing buffer and the complexes were eluted off the magnet in 400 µl of PBS and fixed in 1% formaldehyde in PBS.

These purified complexes were analyzed with an LSRII (BD Biosciences) flow cytometer equipped with 355-, 407-, 488-, 532-, and 638-nm lasers. The background level of fluorescence was evaluated with 0.1 µm filtered PBS, and the threshold was set to the lowest fluorescence channel that did not generate an Alexa Fluor 488 signal with this solution. Based on running fluorescence-free PBS through the cytometer, we set the threshold value to the minimum value that does not generate a signal (~600 to 1,000 fluorescence units measured on the parameter height), which is why the plots displaying the trigger parameter show a straight line in the lower boundary (Supplemental Figure 1). This thresholding allowed us to visualize the fluorescence events associated with virions but not the noise present in virus-free PBS. We defined the gate-eliminating dye aggregates and bead aggregates. In addition, elimination of the high signal height ensures that the signal analyzed remains within the range of linearity of the instrument and below the signal of the compensation controls (Supplemental Figure 1). Spectral compensation coefficients were calculated with the compensation setup feature of DIVA6.1.3 software using CompBeads (BD), either unstained or stained with individual fluorochromes. When compensation controls were acquired, the threshold trigger was set to 5,000 on the FSC channel. When DiO or DiD labels were used, the compensation was set using cells stained with the corresponding dye or unstained cells. For analysis the compensation coefficients were recalculated using FlowJo software (Tree Star). Data were acquired using FACSDiva 6.3 (BD Biosciences) and were analyzed with FlowJo software v9.4.9 (Tree Star).



**Optimization of HIV-1 virion capture.** To optimize the procedure for viral capture, we performed a titration experiment in which we titrated the amounts of both virus and beads. We used gradient-purified viruses and estimated particle content based on the assumption that one viral particle incorporates 5,000 p24 GAG molecules (45).

Based on p24 content, the amount of virus varied between  $4.9 \times 10^9$  and  $1.57 \times 10^6$  virions per assay, and the bead amount varied between  $3.9 \times 10^{12}$  and  $1.25 \times 10^9$  per assay, thus covering a bead/virus ratio from  $2.54 \times 10^{-1}$  to  $2.84 \times 10^6$ . The best recovery for 15-nm MNPs seems to be reached at a bead/virus ratio above  $10^4$ . Since there are around 13 gp120 spikes on HIV-1 virions (46), it is evident that the majority of the beads do not complex with virions. The inability of the beads to bind to virions may be due to the fact that not all of them are coupled with a sufficient number of antibodies to interact with virions with high affinity. Since the beads are revealed by fluorescent GAH Fab fragments against the coupled anti-gp120 antibody, beads that were not coupled with a sufficient amount of anti-gp120 antibodies will not only fail to bind virions, but will also be invisible in flow analysis.

The experiment was conducted by mixing 60  $\mu$ l of virus with 60  $\mu$ l of beads and 3  $\mu$ g of labeled 2G12 antibody; the samples were processed as described above. To minimize variability in sample acquisition and to quantify the number of virions, we acquired a fixed sample volume (160  $\mu$ l) using a high throughput sampler at a flow rate of 0.5  $\mu$ l/s<sup>-1</sup>. We compared the number of viruses recovered and detected by flow virometry to the input viruses estimated by p24 concentration and expressed this as the percentage of recovery. Also, the amount of viral RNA eluted after separation on magnetic columns was compared with the amount that remained attached to the columns, and the amount that flowed through the column was quantified by PCR (see below). In addition, the fractions of HIV-1 that were retained and passed through the column were evaluated by measuring HIV p24 GAG with a sensitive bead assay as described previously (47). Alternatively, we evaluated these fractions using GFP-HIV-1 variants. These virions have been directly visualized and enumerated by flow analysis.

**Capture and detection of HIV-1 virions in body fluids.** In some experiments, HIV virions were analyzed in the context of body fluids, blood plasma, and CVL. Normal blood plasma was obtained from the NIH blood bank. CVL was obtained from M. Gosh (George Washington University, Washington, DC, USA). Blood plasma from HIV-infected individuals was provided by M. Lederman (Case Western Reserve University School of Medicine, Cleveland, Ohio, USA). Both body fluids were obtained according to IRB-approved protocols.

In these experiments, we spiked platelet-poor plasma (PPP) with HIV-1. PPP was obtained from healthy donors' blood collected in 8-ml tubes with sodium citrate (3.2%), centrifuged at 2,000 g for 15 minutes, followed by a second centrifugation at 13,000 g for 2 minutes to remove residual platelets. PPP was spiked with HIV-1<sub>NL4.3</sub> ( $4.9 \times 10^9$  copies/ml) and incubated with MNPs ( $3.9 \times 10^{12}$ ) coupled with VRC01 for 1 hour at 4°C; as a control, we used unspiked plasma. Bound HIV-1<sub>NL4.3</sub> was revealed by another HIV-1 gp120 antibody, 2G12 Alexa 647. MNPs were visualized by staining the Fc portion of the coupled antibody using the Alexa 350 Zenon Labeling Kit (Invitrogen).

To capture HIV-1 in clinical samples, we optimized the protocol described above. PPP containing  $1.1 \times 10^4$  to  $1.6 \times 10^5$  copies/ml of HIV-1 particles was obtained from an infected subject. This concentration was below or close to the cutoff of our standard protocol, which calls for about  $10^5$  copies. Therefore, to concentrate virus, plasma was incubated with MNP-VRC01 capture antibody complexes at 4°C for 1.5 hours. Prior to incubation with plasma, MNPs were stained with the lipophilic dye DiO. MNP-HIV complexes were purified on MS magnetic columns (Miltenyi, Biotec), washed three times with 500  $\mu$ l of washing buffer, and recovered in 200  $\mu$ l of PBS. This eluted fraction was stained with 2G12-A647 in the presence of 2.5% normal mouse serum and incubated for 20 minutes at room temperature. Unbound anti-gp120 antibodies were removed by puri-

fication on  $\mu$ MACS columns; columns were washed four times with 200  $\mu$ l of washing buffer. The MNP-HIV detection antibody complexes were eluted in 200  $\mu$ l of PBS and fixed with 1% formaldehyde in PBS.

**Quantification of HIV-1 virions by RT-PCR.** A 200- $\mu$ l aliquot of the MNP-virus complexes were eluted from a magnetic column, and flowthrough was subjected to nucleic acid extraction on a NucliSENS easyMAG 2.0 instrument (bioMérieux). The columns were treated with the NucliSENS extraction buffer to extract the RNA from viruses that remained attached to the column after elution. Real-time RT-PCR was performed by a one-step RT-PCR with a qScript One-Step Fast MGB qRT-PCR kit (Quanta Biosciences) using a one-step real-time PCR assay with the following primer set: HIV-1 GAG (forward 1): GAGGCTAGAAGGAGAGAGATGGGT, HIV-1 GAG (reverse 1): CCCTGGCCTTAACCGAATTT, and the SR73 probe: FAM-GGG GC GAG AGC GTC AGT ATTA-MGB. Amplifications were carried out on a BioRad CFX96 Touch Thermocycler according to the following cycling parameters: 7.5 minutes at 480°C, 30 seconds at 95°C, followed by 45 cycles of 3 seconds at 95°C and 25 seconds at 600°C.

**Labeling of MNPs and virions for evaluation of coincidences.** MNPs coupled to goat anti-mouse IgG (H+L) antibodies according to the protocol described above were incubated with 3  $\mu$ l of mouse monoclonal antibody labeled either with PE-Cy7 or PE-Cy5.5. Virions were concentrated and separated from serum proteins by centrifugal ultrafiltration on an Amicon ultrafiltration device (Millipore) with a 100K molecular weight cutoff (MWCO), followed by a buffer exchange on the same device with a final volume of 50  $\mu$ l. Viruses were labeled either with Alexa Fluor 350 or Pacific Orange (Invitrogen, Life Technologies) by adding 2.5  $\mu$ l of dye solution (1 mg/ml in DMSO) for 2 hours at room temperature. The labeled viruses were separated from free dyes by ultracentrifugation as described above and reconstituted to their original volumes. Alternatively, washed and concentrated viruses were reconstituted to their original volume with PBS and labeled with the lipophilic fluorescent dyes DiD or DiO (Invitrogen, Life Technologies) at 1.5 and 2.5  $\mu$ M, respectively, in the presence of 0.02% pluronic F-127 (Invitrogen, Life Technologies) for 30 minutes at room temperature. The labeled viruses were washed twice by ultracentrifugation on 30K MWCO centrifugal concentrators to remove free dyes.

**Statistics.** Data normality was verified by the Shapiro-Wilk W test. When the data did not pass the normality test, the nonparametric Wilcoxon procedure was used. When the data were found normally distributed, we used a Student's *t* test to compare two groups of data. All statistical analyses were performed with JMP 9.0 software (SAS Institute). For all statistics, we used two-tailed tests, and a *P* value of less than or equal to 0.05 was considered significant.

**Study approval.** The present study used human material donated by Michael Lederman (plasma) and Mimi Gosh (CVL) obtained in the framework of the studies performed under protocols approved by the IRBs of Case Western University (Cleveland, Ohio, USA) and George Washington University (Washington, DC, USA), respectively.

## Acknowledgments

The authors would like to thank John Mascola for providing VRC01, Tome Hope for providing GFP-expressing HIV-1, Mimi Gosh for providing samples of CVL, and Michael Lederman for providing plasma samples obtained from HIV-1-infected patients. These experiments used reagents provided by the AIDS and Cancer Virus Program, SAIC Frederick, Inc./National Cancer Institute (NCI), Frederick, supported with Federal funds from the NCI, NIH, under contract HHSN261200800001E. We are grateful to Elena Zaitseva for her excellent guidance in staining virions with lipophilic dyes and to Sonia Zicari for her generous help with dengue viruses. We are thankful to Jeremy Swan and Yumiko Shepherd for the preparation of Figure 1. This work was supported by



the intramural program of the Eunice Kennedy-Shriver National Institute of Child Health and Human Development.

Received for publication January 22, 2013, and accepted in revised form June 6, 2013.

Address correspondence to: Leonid Margolis or Jean-Charles Grivel, NIH, 10 Center Drive, Bldg. 10, Rm. 9D58, Bethesda, Maryland 20892, USA. Phone: 301.594.2476; Fax: 301.480.0857; E-mail: margolis@helix.nih.gov (L. Margolis). Phone: 301.594.1298; Fax: 301.480.0857; E-mail: grivelj@mail.nih.gov (J.C. Grivel).

1. Bonner WA, Hulett HR, Sweet RG, Herzenberg LA. Fluorescence activated cell sorting. *Rev Sci Instrum.* 1972;43(3):404–409.
2. Perfetto SP, Chattopadhyay PK, Roederer M. Seven-teen-colour flow cytometry: unravelling the immune system. *Nat Rev Immunol.* 2004;4(8):648–655.
3. Keele BF, et al. Identification and characterization of transmitted and early founder virus envelopes in primary HIV-1 infection. *Proc Natl Acad Sci U S A.* 2008;105(21):7552–7557.
4. Lawn SD, Butera ST. Incorporation of HLA-DR into the envelope of human immunodeficiency virus type 1 in vivo: correlation with stage of disease and presence of opportunistic infection. *J Virol.* 2000; 74(21):10256–10259.
5. Lien KY, Hung LY, Huang TB, Tsai YC, Lei HY, Lee GB. Rapid detection of influenza A virus infection utilizing an immunomagnetic bead-based microfluidic system. *Biosens Bioelectron.* 2011;26(9):3900–3907.
6. Yang SY, Lien KY, Huang KJ, Lei HY, Lee GB. Micro flow cytometry utilizing a magnetic bead-based immunoassay for rapid virus detection. *Biosens Bioelectron.* 2008;24(4):861–868.
7. Stoffel CL, Kathy RF, Rowlen KL. Design and characterization of a compact dual channel virus counter. *Cytometry A.* 2005;65(2):140–147.
8. Steen HB. Flow cytometer for measurement of the light scattering of viral and other submicroscopic particles. *Cytometry A.* 2004;57(2):94–99.
9. Brussaard CP, Marie D, Bratbak G. Flow cytometric detection of viruses. *J Virol Methods.* 2000; 85(1–2):175–182.
10. Hercher M, Mueller W, Shapiro HM. Detection and discrimination of individual viruses by flow cytometry. *J Histochem Cytochem.* 1979;27(1):350–352.
11. Iannelli D, et al. Cytofluorimetric method for the detection of the cucumber mosaic virus. *Phytopathology.* 1996;86:959–965.
12. Iannelli D, et al. Simultaneous detection of cucumber mosaic virus, tomato mosaic virus and potato virus Y by flow cytometry. *J Virol Methods.* 1997; 69(1–2):137–145.
13. Kim BC, Ju MK, Dan-Chin-Yu A, Sommer P. Quantitative detection of HIV-1 particles using HIV-1 neutralizing antibody-conjugated beads. *Anal Chem.* 2009;81(6):2388–2393.
14. Trkola A, et al. Human monoclonal antibody 2G12 defines a distinctive neutralization epitope on the gp120 glycoprotein of human immunodeficiency virus type 1. *J Virol.* 1996;70(2):1100–1108.
15. Zhou T, et al. Structural basis for broad and potent neutralization of HIV-1 by antibody VRC01. *Science.* 2010;329(5993):811–817.
16. Arthur LO, et al. Cellular proteins bound to immunodeficiency viruses: implications for pathogenesis and vaccines. *Science.* 1992;258(5090):1935–1938.
17. Gomez MB, Hildreth JE. Antibody to adhesion molecule LFA-1 enhances plasma neutralization of human immunodeficiency virus type 1. *J Virol.* 1995;69(8):4628–4632.
18. Nguyen DH, Hildreth JE. Evidence for budding of human immunodeficiency virus type 1 selectively from glycolipid-enriched membrane lipid rafts. *J Virol.* 2000;74(7):3264–3272.
19. Ferris MM, McCabe MO, Doan LG, Rowlen KL. Rapid enumeration of respiratory viruses. *Anal Chem.* 2002;74(8):1849–1856.
20. van der Pol E, van Gemert MJ, Sturk A, Nieuwland R, van Leeuwen TG. Single vs. swarm detection of microparticles and exosomes by flow cytometry. *J Thromb Haemost.* 2012;10(5):919–930.
21. Tremblay MJ, Fortin JF, Cantin R. The acquisition of host-encoded proteins by nascent HIV-1. *Immunol Today.* 1998;19(8):346–351.
22. Cantin R, Martin G, Tremblay MJ. A novel virus capture assay reveals a differential acquisition of host HLA-DR by clinical isolates of human immunodeficiency virus type 1 expanded in primary human cells depending on the nature of producing cells and the donor source. *J Gen Virol.* 2001; 82(pt 12):2979–2987.
23. Nyambi PN, Burda S, Bastiani L, Williams C. A virus binding assay for studying the antigenic landscape on intact, native, primary human immunodeficiency virus type 1. *J Immunol Methods.* 2001; 253(1–2):253–262.
24. Leaman DP, Kinkead H, Zwick MB. In-solution virus capture assay helps deconstruct heterogeneous antibody recognition of human immunodeficiency virus type 1. *J Virol.* 2010;84(7):3382–3395.
25. Capobianchi MR, Fais S, Castilletti C, Gentile M, Ameglio F, Dianzani F. A simple and reliable method to detect cell membrane proteins on infectious human immunodeficiency virus type 1 particles. *The J Infect Dis.* 1994;169(4):886–889.
26. Yan X, Schielke EG, Grace KM, Hassell C, Marone BL, Nolan JP. Microsphere-based duplexed immunoassay for influenza virus typing by flow cytometry. *J Immunol Methods.* 2004;284(1–2):27–38.
27. Yan X, Zhong W, Tang A, Schielke EG, Hang W, Nolan JP. Multiplexed flow cytometric immunoassay for influenza virus detection and differentiation. *Anal Chem.* 2005;77(23):7673–7678.
28. Lehmann M, et al. Quantitative multicolor super-resolution microscopy reveals tetherin HIV-1 interaction. *PLoS Pathog.* 2011;7(12):e1002456.
29. Jouvenet N, Zhadina M, Bieniasz PD, Simon SM. Dynamics of ESCRT protein recruitment during retroviral assembly. *Nat Cell Biol.* 2011;13(4):394–401.
30. Jouvenet N, Simon SM, Bieniasz PD. Imaging the interaction of HIV-1 genomes and Gag during assembly of individual viral particles. *Proc Natl Acad Sci U S A.* 2009;106(45):19114–19119.
31. Jouvenet N, Simon SM, Bieniasz PD. Visualizing HIV-1 assembly. *J Mol Biol.* 2011;410(4):501–511.
32. McDonald D, et al. Visualization of the intracellular behavior of HIV in living cells. *J Cell Biol.* 2002;159(3):441–452.
33. Hulme AE, Perez O, Hope TJ. Complementary assays reveal a relationship between HIV-1 uncoating and reverse transcription. *Proc Natl Acad Sci U S A.* 2011;108(24):9975–9980.
34. Lai SK, et al. Human immunodeficiency virus type 1 is trapped by acidic but not by neutralized human cervicovaginal mucus. *J Virol.* 2009; 83(21):11196–11200.
35. Meerloo T, et al. Host cell membrane proteins on human immunodeficiency virus type 1 after in vitro infection of H9 cells and blood mononuclear cells. An immuno-electron microscopic study. *J Gen Virol.* 1993;74(pt 1):129–135.
36. Robey WG, et al. Characterization of envelope and core structural gene products of HTLV-III with sera from AIDS patients. *Science.* 1985;228(4699):593–595.
37. Nolan JP, Stoner SA. A trigger channel threshold artifact in nanoparticle analysis. *Cytometry A.* 2013;83(3):301–305.
38. Zhang X, et al. Cryo-EM structure of the mature dengue virus at 3.5-Å resolution. *Nat Struct Mol Biol.* 2013;20(1):105–110.
39. Gentry MK, Henchal EA, McCown JM, Brandt WE, Dalrymple JM. Identification of distinct antigenic determinants on dengue-2 virus using monoclonal antibodies. *Am J Trop Med Hyg.* 1982; 31(3 pt 1):548–555.
40. Ott DE. Cellular proteins detected in HIV-1. *Rev Med Virol.* 2008;18(3):159–175.
41. Trubey CM, et al. Quantitation of HLA class II protein incorporated into human immunodeficiency virus type 1 virions purified by anti-CD45 immunofluorescence depletion of microvesicles. *J Virol.* 2003; 77(23):12699–12709.
42. Cantin R, Fortin JF, Tremblay M. The amount of host HLA-DR proteins acquired by HIV-1 is virus strain- and cell type-specific. *Virology.* 1996;218(2):372–381.
43. Biancotto A, et al. HIV-1 induced activation of CD4+ T cells creates new targets for HIV-1 infection in human lymphoid tissue ex vivo. *Blood.* 2008; 111(2):699–704.
44. Lawn SD, Roberts BD, Griffin GE, Folks TM, Butera ST. Cellular compartments of human immunodeficiency virus type 1 replication in vivo: determination by presence of virion-associated host proteins and impact of opportunistic infection. *J Virol.* 2000;74(1):139–145.
45. Briggs JA, et al. The stoichiometry of Gag protein in HIV-1. *Nat Struct Mol Biol.* 2004;11(7):672–675.
46. Mao Y, et al. Subunit organization of the membrane-bound HIV-1 envelope glycoprotein trimer. *Nat Struct Mol Biol.* 2012;19(9):893–899.
47. Biancotto A, et al. A highly sensitive and dynamic immunofluorescent cytometric bead assay for the detection of HIV-1 p24. *J Virol Methods.* 2009; 157(1):98–101.